MEANDROS MEDICAL AND DENTAL JOURNAL
September 2024 (3):209-221

Meandros Medical and Dental Journal
doi: 10.69601/meandrosmdj.1540223

Research Article

THIOSTREPTON MODULATES *TLR4* EXPRESSION AND INDUCES APOPTOSIS IN MDA-MB-231 CELLS: AN *IN VITRO* AND *IN SILICO* ANALYSIS

Funda DEMİRTAŞ KORKMAZ [1]*, Zekeriya DÜZGÜN [1], Asuman DEVECİ ÖZKAN [2]

[1]Department of Medical Biology, Faculty of Medicine, Giresun University, Giresun, TURKIYE
[2]Department of Medical Biology, Faculty of Medicine, Sakarya University, Sakarya, TURKIYE
*Correspondence: fundakorkmz@gmail.com

ABSTRACT

Objective: Toll-like receptors (TLRs) are key pattern recognition receptors involved in tumorigenesis, apoptosis, and metastasis. Triple-negative breast cancer (TNBC) is a highly aggressive malignancy, associated with an unfavorable prognosis. Although the role of TLRs in breast cancer remains underexplored, recent studies suggest targeting TLRs in TNBC could be beneficial. In this study Thiostrepton, an antibiotic and novel inhibitor of *TLR7-9* in psoriatic inflammation, was investigated for its effects on *TLR3*, *TLR4*, and *TLR9* expression in TNBC cells (MDA-MB-231).

Materials and Methods: The cytotoxicity of thiostrepton was assessed using the MTT assay. RT-PCR was used to measure gene expression levels of *TLR3*, *TLR4*, *TLR9*, *Bax*, *Bcl-2*, *Nf-κB*, and *E-cadherin*. Cell morphology changes were analyzed with Acridine Orange/Ethidium Bromide (AO/EtBr) staining. Molecular docking and dynamics simulations examined interactions between thiostrepton and the TLR4-MD-2 complex.

Results: Thiostrepton led to a concentration- and time-dependent decrease in cell viability. It significantly inhibited *TLR4*, *Bcl-2* gene expression and increased *TLR3*, *Bax*, and *Nf-κB* levels. The changes in *Bax* and *Bcl-2* gene expression, along with alterations in cell morphology, demonstrated that thiostrepton promoted apoptosis in MDA-MB-231 cells. While *TLR9* expression reduction was not significant, thiostrepton notably increased *TLR3* expression and decreased *TLR4* expression. The three independent molecular dynamics simulations demonstrated that thiostrepton binds stably to the *TLR4-MD2* domain, exhibiting a high binding affinity as indicated by the binding free energy calculations.

Conclusion: Thiostrepton effectively induces apoptosis and reduces cell viability in TNBC cells. *In silico* analysis suggest thiostrepton could modulate *TLR4*, highlighting its potential as a candidate for further research and therapeutic development.

Keywords: Thiostrepton, toll like receptors, TLR4 receptor, triple-negative breast cancer

Received: 28 August 2024
Revised: 24 September 2024
Accepted: 24 September 2024
Published: 29 September 2024

MEANDROS MEDICAL AND DENTAL JOURNAL
September 2024 (3):209-221

Meandros Medical and Dental Journal
doi: 10.69601/meandrosmdj.1540223

INTRODUCTION

Triple-negative breast cancer (TNBC) is a subtype of breast cancer distinguished by the absence of hormone receptors and HER2 expression, which makes it particularly challenging to treat with conventional hormone therapies and HER2-targeted treatments (1). These characteristics contribute to the poor prognosis and difficulty in treating TNBC. Therefore, identifying new targets and therapeutic strategies for TNBC is of paramount importance.

Toll-like receptors (TLRs) are key players in the innate immune system, serving a pivotal function in protecting the body from infections. However, recent research has revealed that TLRs not only manage immune responses but also participate in tumor development, apoptosis, and metastasis (2–4). The role of these receptors, particularly in relation to aggressive breast cancer subtypes such as TNBC, is garnering increasing scientific attention (5,6). It was found that *TLR3* expression is lower in triple-negative breast cancer (TNBC) tissue compared to adjacent normal tissue, and higher *TLR3* expression in TNBC was associated with better prognosis (7). Shi et al. (2020) showed that the expression levels of *TLR4* and *TLR7* significantly affected survival outcomes, with elevated levels correlating with poorer prognosis in breast cancer patients (6). It has been reported that low *TLR9* expression decreases survival in patients with TNBC (8). These findings highlight the complex role of TLRs in breast cancer, suggesting that their expression levels can influence prognosis in different subtypes of the disease. The variation in TLR expression, such as lower *TLR3* and *TLR9* and higher *TLR4* and *TLR7* levels, underscores the need for further research to understand their mechanisms and potential as therapeutic targets.

Molecular docking and Molecular Dynamics (MD) simulations have become indispensable tools in drug discovery and development, offering valuable insights into the interactions between small molecules and their target proteins (9). Molecular docking allows for the prediction of binding modes and affinities of ligands to their receptors, while MD simulations provide a dynamic view of these interactions over time, accounting for the flexibility of both the ligand and the target (10). These computational methods have been successfully employed in various cancer research studies, including those focused on breast cancer, to identify potential drug candidates and elucidate their mechanisms of action (11,12). By combining in silico approaches with experimental data, researchers can accelerate the drug discovery process and gain a deeper understanding of the molecular basis of drug efficacy (13). In the context of TLR-targeted therapies, these computational techniques can offer valuable predictions about the binding of new compounds to TLRs, guiding further experimental investigations and potentially uncovering novel therapeutic strategies.

Thiostrepton, a thiazole antibiotic isolated from *Streptomyces azureus*, is utilized in veterinary medicine but has no clinical applications (14). Recent studies have identified thiostrepton as an inhibitor of the oncogenic transcription factor *FoxM1*, and there is also evidence suggesting that it inhibits *TLR7-9* in psoriatic inflammation (15,16). Several studies have elucidated the antiproliferative, antimetastatic, and

apoptotic effects of thiostrepton in various types of cancer cells (17–19). However, the effects of thiostrepton on TLR expression and its role in challenging cancer types like TNBC are not yet fully understood. This study aims to evaluate the potential of thiostrepton as a therapeutic agent for TNBC by examining its effects on TLRs in TNBC cells. The study combines laboratory experiments (*in vitro*) and computer simulations (*in silico*) to contribute to the identification of novel therapeutic targets and enhance the understanding of thiostrepton's anti-tumor mechanisms.

MATERIALS AND METHODS

Cell culture and treatment process

MDA-MB-231 cell line, representing triple-negative breast cancer, was utilized and sourced from ATCC (USA). Cells were grown in RPMI 1640 medium (Thermo Fisher Scientific, USA), with the addition of 10% fetal bovine serum (FBS, sourced from the US), and supplemented with 100 units/mL penicillin and 100 µg/mL streptomycin (Gibco, Thermo Fisher Scientific, USA). The cultures were kept at 37°C in a humidified incubator with 5% CO2 to promote optimal cell growth and viability. Thiostrepton, procured from Enzo Life Sciences, was dissolved in DMSO to prepare a 10 mM stock solution. DMSO (dimethyl sulfoxide) was sourced from Sigma-Aldrich (St. Louis, MO, USA).

MTT assay

To assess cell viability, cells were seeded into 96-well plates and incubated for 24 hours. After this initial incubation, the cells were treated with thiostrepton concentrations and incubated for an additional 24 or 48 hours. Following the treatment period, MTT solution (5 mg/mL) was added to each well of the plate. Subsequently, the cells were incubated with the MTT reagent for 3 to 4 hours. Following this, the medium was carefully aspirated, and each well received 100 µL of DMSO as a solvent and then plates were placed on an orbital shaker for 3-5 minutes to ensure thorough dissolution. The absorbance of the solution was measured using a spectrophotometer at a wavelength of 540 nm. The viability of the control cells (those not treated with thiostrepton) was defined as 100%, and the viability of the treated cells was calculated as a percentage relative to this control.

Real-time PCR analysis

Total RNA isolation was performed using TRIzol reagent (Invitrogen) with modifications to the method outlined by Chomczynski et al. (20). The Nanodrop spectrophotometer (Thermo Fisher Scientific, Waltham, MA, USA) was used to evaluate the purity and concentration of the isolated RNA. Complementary DNA (cDNA) was subsequently synthesized using the cDNA Reverse Transcription Kit (Thermo Fisher Scientific, Waltham, MA, USA). Real-time PCR amplification was carried out on a

LightCycler instrument (Bio-Rad) with HOT FIREPol EvaGreen qPCR Mix Plus (no ROX) (Solis BioDyne, Inc.) Primers for TLR3, TLR4, TLR9, Bax, Bcl2, Nfkb, E cadherin genes were designed using Oligo7 software. GAPDH was utilized as the endogenous reference gene. Each experiment was conducted in triplicate. Gene expression levels were normalized to GAPDH (ΔCt values), and $2^{-\Delta\Delta Ct}$ method was employed to determine the fold changes in mRNA expression.

Acridine orange/ethidium bromide (AO/EB) staining

AO/EB staining was conducted to assess cell morphology after thiostrepton treatment. Cells ($5x10^5$) were grown in six-well plates and subsequently exposed to 4µM thiostrepton. After 24 hours of incubation, the cell suspension were mixed with AO/EB solution, then cells were dropped on to the microscope slide. Finally, the slides were examined under a fluorescence microscopy (NIKON Eclipse Ni series, Nikon Instruments Inc., USA) at 20x magnification.

Molecular docking

The crystal structure of human TLR4 protein was obtained from the RCSB Protein Data Bank with the PDB code 3FXI (21)(rcsb.org). The thiostrepton compound was obtained from the PubChem database (PubChem CID: 16154490) (22). Molecular docking calculations were analyzed with AutoDock Vina 1.1.2 (23). The calculations were automated using the PyRx software (24). For the docking process, a 17 Å cubic grid box was used, targeting the MD2 triglyceride binding pocket. The resulting protein-compound complex from the docking process was used as the initial structure for molecular dynamics simulations.

Molecular dynamics simulation and free energy calculation

The complex obtained from molecular docking underwent minimization and equilibration phases before being subjected to a 100 ns production run. The process was repeated three times. All simulations were conducted using GROMACS 2020 software (25). The leap-frog integration algorithm was employed in all simulations with 2 fs time step. The AMBER99SB-ILDN force field was used with the TIP3P water model (26). Periodic boundary conditions were applied, and the Particle Mesh Ewald algorithm was employed to handle long-range electrostatics (27).

For the minimization phase, 50,000 steps of the steepest descent algorithm were used with a 10 kJ/mol cutoff . The equilibration phase was conducted in two stages: NVT and NPT ensembles. In the NVT stage, the LINCS algorithm was used as the constraint algorithm, with hydrogen bonds constrained (28). The Verlet cut-off scheme was employed. The Berendsen thermostat was used for temperature coupling, and the simulation length was set to 300 ps (29). In the NPT stage, the V-rescale algorithm was used for temperature coupling, and the Isotropic Berendsen algorithm for pressure coupling (29). The simulation length was set to 1 ns, with the LINCS algorithm applied as in the NVT stage (28).

MEANDROS MEDICAL AND DENTAL JOURNAL
September 2024 (3):209-221

Meandros Medical and Dental Journal
doi: 10.69601/meandrosmdj.1540223

For the production phase, the V-rescale algorithm was used for temperature coupling, and the Isotropic Parrinello-Rahman algorithm for pressure coupling (30). The simulation length was set to 100 ns.

Free energy calculations were performed using the MM-PBSA method with the g_mmpbsa tool (31,32). The polar and apolar components of the solvent effect on free energy were determined using the Poisson-Boltzmann (PB) equation solution and molecular surface area (SA) calculation, respectively. In the vacuum electrostatic calculations, the dielectric constant of the solute was set to 1, while the dielectric constant of the solvent was set to 80. 100 snapshots from the last 10 ns of each 100 ns trajectory were considered in the calculations.

Statistical Analysis

Statistical comparisons between the experimental groups and the control group were performed using a Student's t-test (GraphPad Prism version 10.1.2 for Windows, GraphPad Software, USA). A p-value of less than 0.05 was considered statistically significant.

RESULTS

Evaluating the cytotoxic and cellular effects of thiostrepton on MDA-MB-231 cells

Figure 1A illustrates the changes in cell viability percentages of MDA-MB-231 cells following incubation with thiostrepton for 24 and 48 hours.

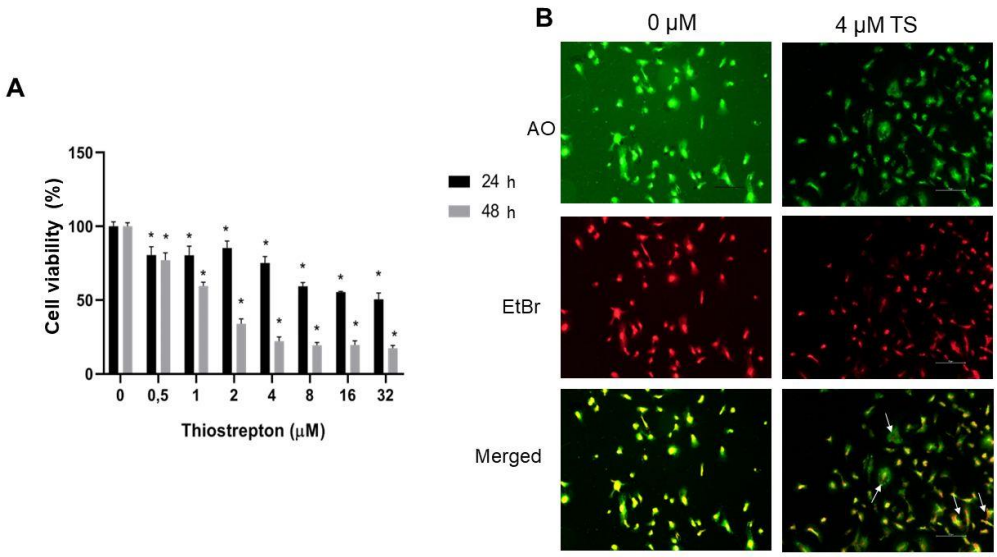

Figure 1. A) MTT assay results illustrating cell viability at different thiostrepton concentrations over 24 and 48 hours. Each value represents the mean ± SEM of four experiments (*p < 0.05). B) Morphologic examination with AO/EB staining after MDA-MB-231 cells were treated with 4 µM thiostrepton for 24 h (↗ indicates apoptotic cells).

MEANDROS MEDICAL AND DENTAL JOURNAL
September 2024 (3):209-221

Meandros Medical and Dental Journal
doi: 10.69601/meandrosmdj.1540223

Thiostrepton decreased cell viability, which was both dose- and time-dependent, indicating its potent cytotoxic effect on MDA-MB-231 cells. Cell viability decreased dramatically at thiostrepton concentrations of 2 μM and above, especially following 48 hours of treatment. Briefly, 16 μM and 32 μM thiostrepton treatments for 48 hours resulted in about 20% and 10% of cell growth inhibition in MDA-MB-231 cells. Additionally, it was observed that thiostrepton disrupted the membrane and nuclear integrity of the cells and altered cell morphology in an apoptotic manner (Figure 1B). These findings collectively support the potential of thiostrepton as effective agent in promoting apoptosis and inhibiting cancer cell proliferation.

Effects of thiostrepton treatment on Toll-like receptors and apoptotic genes

Thiostrepton treatment reduced the expression of *TLR4*, *TLR9*, *Bcl-2*, and *E-cadherin* by 0.29, 0.61-, 0.23-, and 0.63-fold, respectively, while it increased the expression levels of *TLR3*, *Bax*, and *NF-κB* by 2.19-, 3.17-, and 2.87-fold, respectively (Figure 2). Although the reduction in TLR9 expression was not statistically significant, there was a notable decrease in *TLR4* expression. In contrast, *TLR3* expression was significantly upregulated. Despite the significant increase in *NF-κB* expression, no significant change was detected in *E-cadherin* expression. The pro-apoptotic gene *Bax* was significantly upregulated, while the anti-apoptotic gene *Bcl-2* was markedly downregulated. These results indicate that thiostrepton plays a significant regulatory role in modulating apoptotic pathways and inflammatory responses.

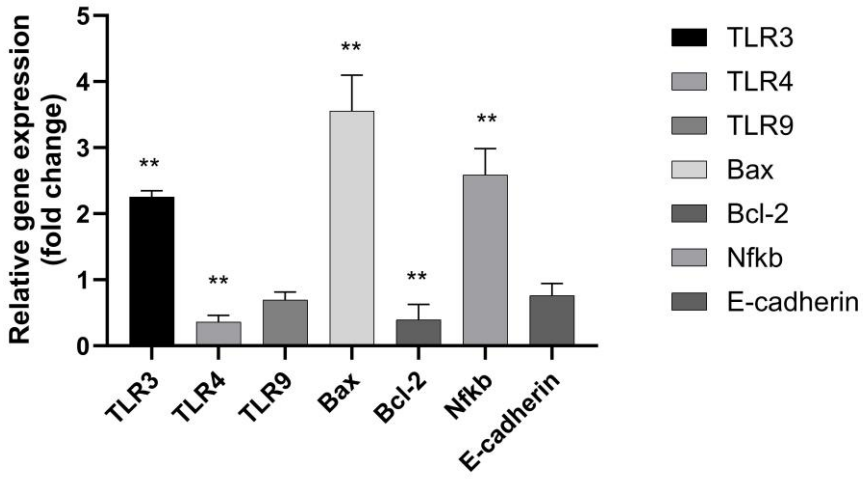

Figure 2. Relative gene expression levels of genes after treating MDA-MB-231 cells with 4 μM thiostrepton for 24 hours. Expression levels were standardized against *β-actin* mRNA levels (** $p < 0.01$).

Molecular dynamics simulation and free energy calculation on TLR4

Our molecular dynamics (MD) simulations of the *TLR4-MD2* domain in complex with thiostrepton provide valuable insights into the stability and interactions of this system. The 100 ns simulations, replicated three times, revealed several interesting features of the complex's behavior over time.

MEANDROS MEDICAL AND DENTAL JOURNAL
September 2024 (3):209-221

Meandros Medical and Dental Journal
doi: 10.69601/meandrosmdj.1540223

The RMSD analysis (Figure 3A), demonstrated that thiostrepton maintained remarkable stability within the binding cavity throughout the simulation. This stability suggests a strong affinity between the compound and its binding site, which could be indicative of its potential as a *TLR4-MD2* modulator. However, the protein itself showed some interesting dynamics, with a partial loss of stability observed from approximately 75 ns onwards, followed by a return to stability as the simulation approached 100 ns. This transient instability could represent a conformational shift in the protein, possibly induced by the presence of thiostrepton.

The radius of gyration analysis (Figure 3B) corroborated our RMSD findings, showing partial conformational changes in the protein structure from around 60 ns. This observation further supports the idea of thiostrepton-induced conformational shifts in the *TLR4-MD2* complex. The RMSF plot (Figure 3C) revealed that the MD2 domain exhibited greater flexibility compared to other regions of the TLR4 protein. This increased mobility of MD2 could be crucial for accommodating ligands and initiating signaling cascades.

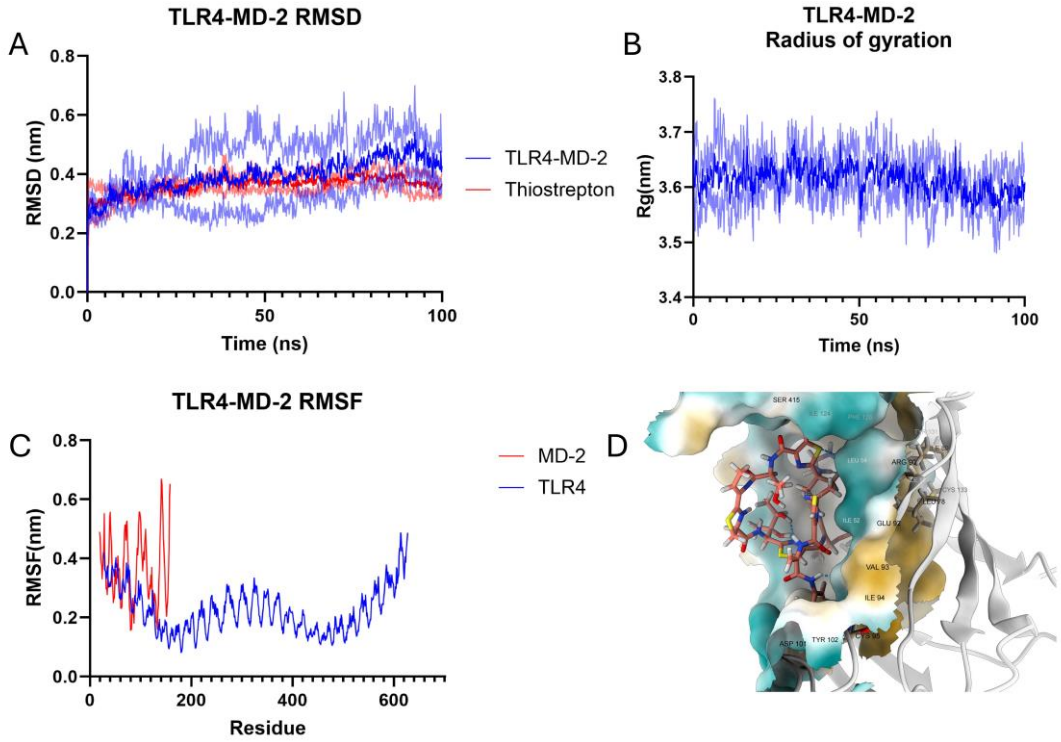

Figure 3. RMSD, Radius of gyration, and RMSF plots of Thiostrepton and TLR4-MD2 domain after 100 ns MD simulation with 3 replicates (A,B,C), and 3D representation of protein-compound interaction (D)

Detailed examination of the thiostrepton-MD2 interaction at the atomic level (Figure 3D) revealed specific residues involved in hydrogen bonding, namely Arg90, Val93, and Cys95. These interactions likely

contribute to the observed stability of thiostrepton within the binding cavity throughout the simulation. This information could be valuable for structure-based drug design efforts targeting the *TLR4-MD2* complex.

The molecular mechanics Poisson-Boltzmann surface area (MM/PBSA) calculations for the binding free energies of the TLR4-MD2 domain and thiostrepton revealed remarkably low values ranging from -319.7 to -403.09 kJ/mol (Table 1). These exceptionally favorable binding energies suggest a strong affinity between thiostrepton and the TLR4-MD2 complex, indicating potential biological significance in their interaction.

Table 1. Binding free energies and contributions between TLR4 MD2 domain and thiostrepton at the end of 100 ns according to the MM/PBSA method

	Repeat-1		Repeat-2		Repeat-3	
	Mean (kJ/mol)	**Std. E (kJ/mol)**	**Mean (kJ/mol)**	**Std. E (kJ/mol)**	**Mean (kJ/mol)**	**Std. E (kJ/mol)**
Van der Waals	-427.325	2.616	-245.643	1.46	-277.803	1.837
Electrostatic	-325.151	4.633	-502.786	4.304	-306.616	3.461
Polar solvation	397.704	6.477	454.738	3.831	245.969	4.352
SASA	-47.821	0.241	-26.069	0.142	-36.217	0.197
Binding energy	-403.09	3.276	-319.7	3.455	-374.687	2.618

A detailed analysis of the energetic contributions revealed that van der Waals interactions were the predominant force driving this binding, with a minimum contribution of -427 kJ/mol. This substantial van der Waals contribution underscores the importance of non-covalent interactions in stabilizing the thiostrepton-TLR4-MD2 complex. Such strong van der Waals interactions often indicate a good shape complementarity between the ligand and the binding pocket, which could be crucial for the compound's potential modulatory effects on *TLR4* signaling.

DISCUSSION

Thiostrepton, a polypeptide antibiotic, was first isolated from *Streptomyces azureus* in 1954 and was primarily recognized for its inhibition of protein synthesis (14). It was discovered that siomycin A, a thiazole antibiotic structurally similar to thiostrepton, could downregulate the oncogenic transcription factor FoxM1 in cancer cells (33). This effect was later observed with thiostrepton, leading to a reduction in anchorage-independent growth of cancer cells. Studies demonstrated that thiostrepton selectively induced cell cycle arrest and apoptosis in breast cancer cells by downregulating *FoxM1* expression (19,34,35). In the literature, thiostrepton is also recognized as an inhibitor of *TLR7-9* in psoriatic inflammation. However, the interactions between thiostrepton and these receptors are not well understood (36). Therefore, we investigated the effects of thiostrepton on *TLR3*, *TLR4*, and *TLR9* in MDA-MB-231 breast cancer.

Studies conducted on various breast cancer and other cancer cell lines have reported IC50 values for thiostrepton ranging from 1 to 5 μM (15,19,35). In our study, cell viability at 8 μM thiostrepton concentration

was 55% after 24 hours, while for the 48-hour treatment, cell viability dropped below 50% at concentrations above 2 μM. These findings align with the existing literature, suggesting that thiostrepton exhibits significant cytotoxicity in TNBC cells. Although thiostrepton has been recognized for its significant effects in cancer cells, its cytotoxic and genotoxic effects on non-malignant healthy cells remain largely unexplored. Therefore, it is imperative that further investigations be conducted to elucidate the cytotoxic effects of thiostrepton on healthy cells.

The significant increase in the expression of *Bax*, a pro-apoptotic gene, indicates that thiostrepton triggers apoptotic pathways, leading to cell death. The decrease in *Bcl-2*, an anti-apoptotic gene, when considered alongside the increase in *Bax*, strongly suggests that thiostrepton promotes cell death by activating apoptotic signaling pathways. Studies have shown that thiazole antibiotics such as siomycin A and thiostrepton induce apoptosis in various types of cancer cells (17,37). Liu et al. found that thiostrepton markedly decreased the proliferation of gastric cancer cells and caused both G0/G1 phase cell cycle arrest and apoptosis (38). Kuttikrishnan et al. reported that downregulation of the *FoxM1/SKP2/MTH1* pathway through thiostrepton resulted in an increased *Bax/Bcl2* ratio and the suppression of anti-apoptotic proteins (39). Along with all these findings, changes in cell morphology and *Bax/Bcl-2* gene expression in our study confirm that thiostrepton induces apoptosis.

The 2.87-fold increase in *NF-κB* expression induced by thiostrepton may indicate activation of cellular inflammatory responses and survival pathways. Peng et al. showed that after incubation with thiostrepton, *NF-κB* activation was observed in latently infected Bcl-2-transduced CD4+ T cells (40). Lai et al. also reported that thiostrepton does not suppress *NF-κB* activation induced by *TNF-α*, *IL-1*, or other Toll-like receptor (TLR) stimuli (41). Although it has been shown that thiostrepton increases *E-cadherin* expression in cancer cells, our study did not observe a significant change in *E-cadherin* expression (19,42).

TLR3 was shown to trigger apoptosis through the TRIF adaptor protein and type I interferon (IFN) autocrine signaling. It was also noted that *IL-1R-associated kinase-4 (IRAK-4)* and *NF-κB* play key roles in the *TLR3*-mediated apoptotic signaling, leading to the activation of extrinsic caspases (43,44). According to our findings, the increased expression of Toll-like receptor 3 (TLR3) suggests that thiostrepton treatment may activate immune responses, thereby enhancing cellular responses to apoptosis.

Some studies have reported that thiostrepton is a *TLR7-9* inhibitor (41,45). In our study, although a reduction in *TLR9* expression was observed, it was not found to be statistically significant. However, the substantial suppression of *TLR4* expression by thiostrepton is particularly noteworthy. To our knowledge, no studies have examined the effects of thiostrepton on *TLR4*. Consequently, we sought to investigate whether thiostrepton exerts an effect on TLR4 by conducting molecular dynamics and docking studies.

Interestingly, our study appears to be the first to investigate the interaction between thiostrepton and the *TLR4-MD2* complex using MD simulations. This novelty highlights the potential for new insights into *TLR4* modulation. Our findings can be contextualized within the broader literature on *TLR4-MD2*

interactions. For instance, Niu et al. (2018) conducted a similar study with ursolic acid, demonstrating its ability to bind to MD2's active pocket and alter *TLR4* conformation, ultimately reducing *TLR4-MD2* activity. The gradual loss of protein stability observed in their study aligns with our findings, suggesting that this may be a common feature in *TLR4-MD2* interactions with small molecules (46).

To contextualize our findings, it is instructive to compare them with related studies in the literature. For instance, Sun et al. conducted a comprehensive study on PCP-W1, a polysaccharide isolated from *Poria coco*s. Their research encompassed structural analysis, investigation of immunomodulatory effects in RAW 264.7 cells, and *in silico* studies including molecular docking and molecular dynamics simulations to elucidate the binding mechanism of PCP-W1 to the TLR4/MD2 complex. Their findings demonstrated that PCP-W1 induced M1-type macrophage polarization via the TLR4/MD2/NF-κB pathway. Notably, their computational analysis yielded a binding free energy of -288.23 kJ/mol for the interaction between PCP-W1 and MD2 (47).

When juxtaposed with our results, it becomes evident that thiostrepton exhibits a more favorable binding affinity to the TLR4-MD2 complex compared to PCP-W1. The lower (more negative) binding free energy we observed for thiostrepton suggests a potentially stronger interaction with the TLR4-MD2 complex. This enhanced binding affinity could translate to more potent modulation of TLR4-mediated signaling pathways.

However, it is crucial to interpret these computational findings with caution. While binding free energy calculations provide valuable insights into the thermodynamics of protein-ligand interactions, they do not always directly correlate with biological activity. Factors such as bioavailability, off-target effects, and the complex cellular milieu can significantly influence a compound's efficacy *in vivo*.

Furthermore, the structural differences between thiostrepton (a cyclic oligopeptide) and PCP-W1 (a polysaccharide) should be considered when comparing their binding energies. These distinct molecular architectures may interact with the *TLR4-MD2* complex through different mechanisms, potentially activating or inhibiting diverse downstream signaling cascades.

CONCLUSION

This study demonstrated that thiostrepton promotes apoptosis and reduces cell viability in TNBC cells. Additionally, for the first time in the literature, it showed the effects of thiostrepton on *TLR4* gene expression and its interaction with the *TLR4-MD2* complex using MD simulations. However, there are several suggestions for more detailed analysis of these results. While our simulations provide important computational insights, it is crucial to acknowledge the limitations of this approach. MD simulations, while powerful, represent a simplified model of complex biological systems. Therefore, experimental validation of these findings would be a logical next step. Extending the simulation time beyond 100 ns could potentially

reveal longer-term dynamics of the system. Moreover, to validate the biological relevance of the *in vitro* and *in silico* findings, the effects of thiostrepton on *TLR4* should be examined in different TNBC cell lines or animal models *in vivo.*

Acknowledgments

None

Authorship contributions

F.D.K; Conceptualization, Methodology, Writing—Original Draft. Z.D.; Methodology, Writing Original Draft. A.D.O; Conceptualization, Methodology, Supervision.

Data availibity statement

The data that support the findings of this study are available from the corresponding author upon reasonable request.

Declaration of competing interest

No conflict of interest was declared by the authors

Ethics

This study does not contain any experiments with human participants or animals conducted by the authors.

Funding

This work has not received any funding support.

REFERENCES

1. Foulkes WD, Smith IE, Reis-Filho JS. Triple-Negative Breast Cancer. N Engl J Med. 2010;363(20):1938–48.
2. Javaid N, Choi S. Toll-like Receptors from the Perspective of Cancer Treatment. Cancers 2020;12(2):297.
3. Rakoff-Nahoum S, Medzhitov R. Toll-like receptors and cancer. Nat Rev Cancer. 2009;9(1):57–63.
4. Ren T, Wen ZK, Liu ZM, Liang YJ, Guo ZL, Xu L. Functional expression of TLR9 is associated to the metastatic potential of human lung cancer cell. Cancer Biol Ther. 2007;6(11):1704-1709.
5. Butkowsky C, Aldor N, Poynter SJ. Toll-like receptor 3 ligands for breast cancer therapies (Review). Mol Clin Oncol. 2023;19(2):1-8.
6. Shi S, Xu C, Fang X, Zhang Y, Li H, Wen W, et al. Expression profile of Toll-like receptors in human breast cancer. Mol Med Rep. 2020; 21(2):786-794.
7. Fan L, Sui XY, Jin X, Zhang WJ, Zhou P, Shao ZM. High expression of TLR3 in triple-negative breast cancer predicts better prognosis—data from the Fudan University Shanghai Cancer Center cohort and tissue microarrays. BMC Cancer. 2023;23(1):298.
8. Tuomela J, Sandholm J, Karihtala P, Ilvesaro J, Vuopala KS, Kauppila JH, et al. Low TLR9 expression defines an aggressive subtype of triple-negative breast cancer. Breast Cancer Res Treat. 2012;135(2):481-493.
9. Ahmed M, Maldonado AM, Durrant JD. From byte to bench to bedside: molecular dynamics simulations and drug discovery.

BMC Biol. 2023;21(1):299.
10. Salo-Ahen OMH, Alanko I, Bhadane R, Bonvin AMJJ, Honorato RV, Hossain S, et al. Molecular dynamics simulations in drug discovery and pharmaceutical development. Processes. 2020;9(1):71.
11. Muhammed MT, Aki-Yalcin E. Molecular docking: principles, advances, and its applications in drug discovery. Lett Drug Des Discov. 2024;21(3):480–95.
12. Nascimento IJ dos S, de Aquino TM, da Silva-Júnior EF. The new era of drug discovery: The power of computer-aided drug design (CADD). Lett Drug Des Discov. 2022;19(11):951–5.
13. Ain Q ul, Batool M, Choi S. TLR4-targeting therapeutics: structural basis and computer-aided drug discovery approaches. Molecules. 2020;25(3):627.
14. Bailly C. The bacterial thiopeptide thiostrepton. An update of its mode of action, pharmacological properties and applications. Eur J Pharmacol. 2022;914:174661.
15. Bhat UG, Halasi M, Gartel AL. Thiazole antibiotics target FoxM1 and induce apoptosis in human cancer cells. PLoS One. 2009;4(5):e5592.
16. Lai C-Y, Yeh D-W, Lu C-H, Liu Y-L, Huang L-R, Kao C-Y, et al. Identification of Thiostrepton as a Novel Inhibitor for Psoriasis-like Inflammation Induced by TLR7–9. J Immunol. 2015;195(8).
17. Kwok JMM, Myatt SS, Marson CM, Coombes RC, Constantinidou D, Lam EWF. Thiostrepton selectively targets breast cancer cells through inhibition of forkhead box M1 expression. Mol Cancer Ther. 2008;7(7):2022–32.
18. Cai X, Xiao W, Shen J, Lian H, Lu Y, Liu X, et al. Thiostrepton and miR-216b synergistically promote osteosarcoma cell cytotoxicity and apoptosis by targeting FoxM1. Oncol Lett [Internet]. 2020;20(6):1–1.
19. Demirtas Korkmaz F, Dogan Turacli I, Esendagli G, Ekmekci A. Effects of thiostrepton alone or in combination with selumetinib on triple-negative breast cancer metastasis. Mol Biol Rep [Internet]. 2022;49(11):10387–97.
20. Chomczynski P, Sacchi N. Single-step method of RNA isolation by acid guanidinium thiocyanate-phenol-chloroform extraction. Anal Biochem. 1987;162(1):156-159.
21. Park BS, Song DH, Kim HM, Choi B-S, Lee H, Lee J-O. The structural basis of lipopolysaccharide recognition by the TLR4–MD-2 complex. Nature. 2009;458(7242):1191–5.
22. Kim S, Thiessen PA, Bolton EE, Chen J, Fu G, Gindulyte A, et al. PubChem Substance and Compound databases. Nucleic Acids Res. 2016;44(D1):D1202–13.
23. Trott O, Olson AJ. AutoDock Vina: improving the speed and accuracy of docking with a new scoring function, efficient optimization, and multithreading. J Comput Chem. 2010;31(2):455–61.
24. Dallakyan S, Olson AJ. Small-Molecule Library Screening by Docking with PyRx. In 2015 p. 243–50.
25. Abraham MJ, Murtola T, Schulz R, Páll S, Smith JC, Hess B, et al. GROMACS: High performance molecular simulations through multi-level parallelism from laptops to supercomputers. SoftwareX. 2015;1–2:19–25.
26. Lindorff-Larsen K, Piana S, Palmo K, Maragakis P, Klepeis JL, Dror RO, et al. Improved side-chain torsion potentials for the Amber ff99SB protein force field. Proteins. 2010;78(8):1950–8.
27. Essmann U, Perera L, Berkowitz ML, Darden T, Lee H, Pedersen LG. A smooth particle mesh Ewald method. J Chem Phys. 1995;103(19):8577.
28. Hess B, Bekker H, Berendsen HJC, Fraaije JGEM. LINCS: A Linear Constraint Solver for Molecular Simulations. J Comput Chem. 1997;18:1463–72.
29. Lemak AS, Balabaev NK. On the Berendsen thermostat. Mol Simul. 1994;13(3):177–87.
30. Martoňák R, Laio A, Parrinello M. Predicting Crystal Structures: The Parrinello-Rahman Method Revisited. Phys Rev Lett. 2003;90(7): 075503.
31. Wang E, Sun H, Wang J, Wang Z, Liu H, Zhang JZH, et al. End-Point Binding Free Energy Calculation with MM/PBSA and MM/GBSA: Strategies and Applications in Drug Design [Internet]. Vol. 119, Chemical Reviews. American Chemical Society.2019 p. 9478–508.
32. Kumari R, Kumar R, Lynn A, Lynn A. g_mmpbsa—A GROMACS Tool for High-Throughput MM-PBSA Calculations. J Chem Inf Model. 2014;54(7):1951–62.
33. Gartel AL. FoxM1 inhibitors as potential anticancer drugs. Expert Opin Ther Targets. 2008;12(6):663–5.
34. Wongkhieo S, Numdee K, Lam EWF, Choowongkomon K, Kongsema M, Khongkow M. Liposomal Thiostrepton Formulation and Its Effect on Breast Cancer Growth Inhibition. J Pharm Sci. 2021;110(6):2508–16.
35. Kongsema M, Wongkhieo S, Khongkow M, Lam E, Boonnoy P, Vongsangnak W, et al. Molecular mechanism of Forkhead box M1 inhibition by thiostrepton in breast cancer cells. Oncol Rep . 2019;42(3):953–62.
36. Lai CY, Su YW, Lin KI, Hsu LC, Chuang TH. Natural Modulators of Endosomal Toll-Like Receptor-Mediated Psoriatic Skin Inflammation. Journal of Immunology Research. 2017;2017:1-15.

37. Jiang L, Wang P, Chen L, Chen H. Down-regulation of FoxM1 by thiostrepton or small interfering RNA inhibits proliferation, transformation ability and angiogenesis, and induces apoptosis of nasopharyngeal carcinoma cells. Int J Clin Exp Pathol. 2014;7(9):5450–60.
38. Liu SX, Zhou Y, Zhao L, Zhou LS, Sun J, Liu GJ, et al. Thiostrepton confers protection against reactive oxygen species-related apoptosis by restraining FOXM1-triggerred development of gastric cancer. Free Radic Biol Med. 2022 20;193:385–404.
39. Kuttikrishnan S, Prabhu KS, Khan AQ, Alali FQ, Ahmad A, Uddin S. Thiostrepton inhibits growth and induces apoptosis by targeting FoxM1/SKP2/MTH1 axis in B-precursor acute lymphoblastic leukemia cells. Leuk Lymphoma. 2021;62(13):3170–80.
40. Peng W, Hong Z, Chen X, Gao H, Dai Z, Zhao J, et al. Thiostrepton reactivates latent HIV-1 through the p-TEFb and NF-κB pathways mediated by heat shock response. Antimicrob Agents Chemother. 2020;64(5):10-1128..
41. Lai C-Y, Yeh D-W, Lu C-H, Liu Y-L, Huang L-R, Kao C-Y, et al. Thiostrepton inhibits psoriasis-like inflammation induced by TLR7, TLR8, and TLR9. J Immunol. 2016 1;196(1_Supplement):124.41.
42. Hsu Y Bin, Lan MC, Kuo YL, Huang CYF, Lan MY. A preclinical evaluation of thiostrepton, a natural antibiotic, in nasopharyngeal carcinoma. Invest New Drugs. 2020;38(2): 264-273.
43. Salaun B, Coste I, Rissoan M-C, Lebecque SJ, Renno T. TLR3 Can Directly Trigger Apoptosis in Human Cancer Cells. J Immunol. 2006;176(8):4894–901.
44. Butkowsky C, Aldor N, Poynter S. Toll-like receptor 3 ligands for breast cancer therapies (Review). Mol Clin Oncol. 2023;19(2):1-8.
45. Esparza K, Oliveira SD, Castellon M, Minshall RD, Onyuksel H. Thiostrepton-Nanomedicine, a TLR9 Inhibitor, Attenuates Sepsis-Induced Inflammation in Mice. Yokota S, editor. Mediators Inflamm. 2023;2023:1–11.
46. Niu X, Yu Y, Guo H, Yang Y, Wang G, Sun L, et al. Molecular modeling reveals the inhibition mechanism and binding mode of ursolic acid to TLR4-MD2. Comput Theor Chem. 2018;1123:73–8.
47. Sun M, Yao L, Yu Q, Duan Y, Huang J, Lyu T, et al. Screening of Poria cocos polysaccharide with immunomodulatory activity and its activation effects on TLR4/MD2/NF-κB pathway. Int J Biol Macromol. 2024;273:132931.